

## Scanning tunneling microscopy investigation of the TiO<sub>2</sub> anatase (101) surface

Wilhelm Hebenstreit,<sup>1</sup> Nancy Ruzycki,<sup>1</sup> Gregory S. Herman,<sup>2</sup> Yufei Gao,<sup>2</sup> and Ulrike Diebold<sup>1,\*</sup>

<sup>1</sup>Department of Physics, Tulane University, New Orleans, Louisiana 70118

<sup>2</sup>Environmental Molecular Sciences Laboratory, Pacific Northwest National Laboratory, PO Box 999, MSIN K8-93, Richland, Washington 99352

(Received 10 October 2000)

We report the first scanning tunneling microscopy (STM) study of single-crystalline anatase. Atomically resolved images of the (101) surface are consistent with a bulk-truncated (1×1) termination. Step edges run predominantly in the [010], [ $\bar{1}11$ ], and [ $\bar{1}\bar{1}1$ ] directions. The surface is stable with very few point defects. Fourfold-coordinated Ti atoms at step edges are preferred adsorption sites and allow the identification of tunneling sites in STM.

Titanium dioxide (TiO<sub>2</sub>) is a versatile material that finds uses as a promoter in heterogeneous catalysis, gas sensor, in protective and optically active coatings, as a pigment in paints, and most importantly, as a promising photoactive material in the photocatalytic degradation of environmental pollutants<sup>1,2</sup> and in solar cells.<sup>3</sup> TiO<sub>2</sub> exists in the three common crystallographic phases, rutile, anatase, and brookite. Commercial TiO<sub>2</sub> powder catalysts are a mixture of rutile and anatase and, for reasons not yet completely understood, anatase is the more photocatalytically active form.<sup>1</sup> Many detailed surface investigations have been performed on single-crystalline rutile TiO<sub>2</sub> in order to understand, and ultimately control, the surface chemistry underlying all these applications. A rather complete understanding of the surface properties of rutile has evolved.<sup>4</sup> In comparison, relatively little is known about the surface properties of the technologically more important anatase phase, mainly for lack of appropriate single-crystalline specimens.

In crystalline powder materials, the (101) and the (100)/(010) anatase surface planes are typically found, together with some (001). Calculated surface energies are 0.52 and 0.81 J/m<sup>2</sup> for anatase (101) and (001), respectively, and 0.82 J/m<sup>2</sup> for the thermodynamically most stable rutile surface, (110).<sup>5</sup> The rutile (110) (1×1) surface undergoes a (1×2) reconstruction after annealing to high temperatures under reducing conditions.<sup>6</sup> The surfaces of anatase (001) were found to undergo a (1×4) reconstruction upon sputtering and annealing in ultrahigh vacuum (UHV).<sup>7,8</sup> We are aware of only one study with surface science techniques of an anatase (101) surface.<sup>8</sup> Electron-diffraction patterns consistent with an unreconstructed (1×1) termination were observed, but any details of the surface geometry, morphology, and electronic structure of clean anatase (101) are unknown. Hence the scanning tunneling microscopy (STM) results in this paper should present an important starting point for molecular-level research involving anatase surfaces.

Stable oxide surfaces are typically autocompensated or nonpolar,<sup>9</sup> and their surface structures can be predicted with simple electron-counting rules. For TiO<sub>2</sub> the same number of Ti→O as O→Ti bonds have to be broken when cutting a TiO<sub>2</sub> crystal along a certain direction in a structural analysis. A model of the autocompensated, bulk-terminated (101) sur-

face is shown in Fig. 1. It exhibits a sawtooth structure with twofold-coordinated oxygen ions at [010]-oriented ridges. The other oxygen ions are threefold coordinated as in the bulk. The coordination of the surface Ti ions are sixfold and fivefold. In the bulk Ti ions are sixfold coordinated.

The sample was a natural anatase single crystal 14×8×8 mm<sup>3</sup> in size and metallic opaque in color. X-ray photoelectron spectroscopy (XPS) indicated small amounts of impurities (Zr, Al, Zn, and Pb). In order to achieve a clean surface, a 700-Å thick epitaxial TiO<sub>2</sub> film was grown with oxygen plasma assisted molecular-beam epitaxy. *In situ* characterization with reflection high-energy electron diffraction gave sharp streaks with no higher-order features suggesting a flat film with a bulklike (1×1) termination. Furthermore, *in situ* Ti 2*p* XPS results indicated the presence of only Ti<sup>4+</sup>.<sup>15</sup> The STM experiments were performed at room temperature in a separate UHV chamber. After transport through air the sample was cleaned by sputtering (1000 eV Ar<sup>+</sup>, 1 μA/cm<sup>2</sup>) and annealing until a sharp (1×1) low-

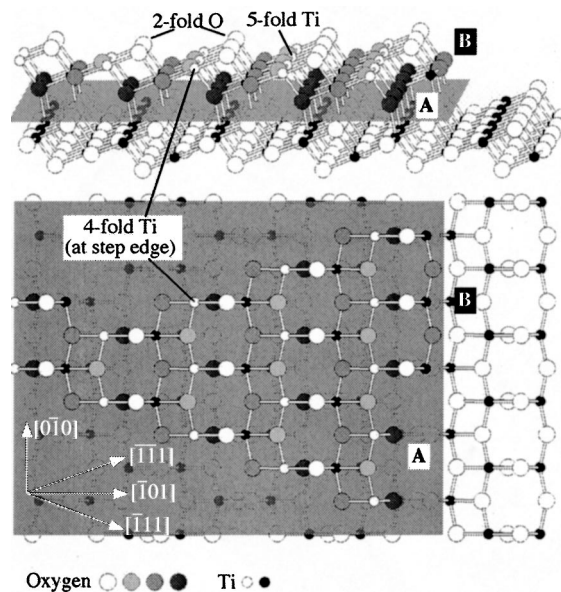


FIG. 1. Atomic model of an anatase (101)(1×1) surface, top, and side view. The two possible terminations for step edges along [010] are indicated by A and B.

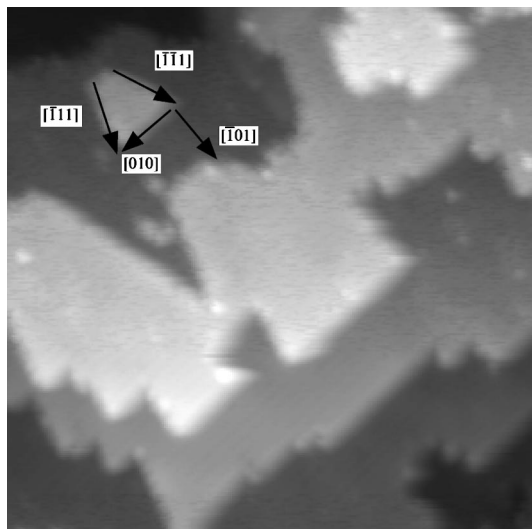


FIG. 2. STM image ( $V_{sample} = +1.5$  V,  $I_{tunnel} = 1$  nA,  $250 \times 250 \text{ \AA}^2$ ) of anatase (101) showing preferential orientations of monoatomic step edges.

energy electron-diffraction (LEED) pattern was regained. It is well known that anatase transforms into rutile at high temperature, and heating to  $650^\circ\text{C}$  was deemed safe to avoid this phase transition. No impurities were observed, except for a small Mg peak in low-energy ion scattering. A rutile (110) sample was prepared with standard preparation procedures<sup>10</sup> and used for comparison.

The surface was not of uniformly good quality, but on certain areas a clear terrace/step structure was observed with STM. It showed  $\sim 100 \text{ \AA}$  high “hills” consisting  $\sim 100 \text{ \AA}$  wide terraces, separated by  $4 \text{ \AA}$  high, monoatomic steps (Fig. 2). The annealing temperature was probably not high enough for the formation of larger terraces. Three step orientations are clearly preferred, giving rise to the triangularly shaped island in Fig. 2. The [010] orientation is easily identified in atomically resolved STM images and LEED. Note that the two perpendicular directions,  $[\bar{1}01]$  and  $[10\bar{1}]$ , are inequivalent, running with or against the “sawtooths,” respectively. Their orientation on the sample can be identified from the typical island shape and considerations concerning the stability of step edges. The same rule that is used for predicting autocompensated  $\text{TiO}_2$  surfaces (i.e., the number of broken bonds at Ti atoms equals the number of broken bonds at O atoms), can also be applied to predict stable step geometries. The predominant step orientations on rutile (110) are consistent with this concept.<sup>10</sup> The top surface of the anatase model in Fig. 1 is shaped as a triangular island. It is bordered by a [010] step and two autocompensated step edges that include the experimentally observed angles with [010]. A mirror-symmetric island would have step edges along  $[\bar{1}11]$  and  $[\bar{1}\bar{1}1]$  at the upper and lower side, respectively. Such steps are not autocompensated and are not observed in Fig. 2. Two different terminations are possible for the [010] step. Based on the inspection of several STM images the step edges labeled A seem to be favored.

The four-fold coordinated Ti atoms exposed on  $[\bar{1}11]$ , and  $[\bar{1}\bar{1}1]$ -oriented step edges (Fig. 1) should be favored as binding sites for adsorbed atoms or molecules. Single bright

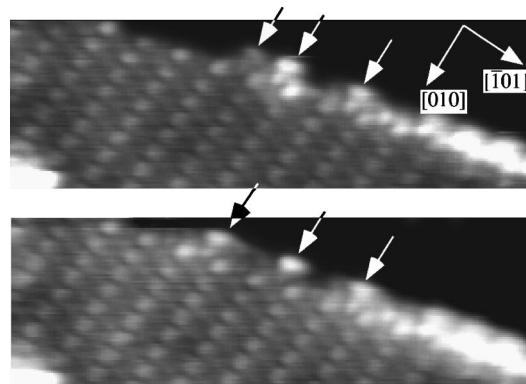


FIG. 3. Consecutive STM images ( $V_{sample} = +0.91$  V,  $I_{tunnel} = 12$  nA,  $73 \times 23 \text{ \AA}^2$ ). The bright spots marked with arrows are presumably adsorbates. The upper one is at different positions in the two images.

spots are often observed on these steps (Fig. 3). Sometimes, a spot switches over to an equivalent site during consecutive STM images (Fig. 3), indicating that these are indeed adsorbates which are either moved by the STM tip or hop spontaneously. Their composition cannot be determined since the concentration is well below the detection limit of standard surface analytical techniques. Nevertheless, their presence supports the proposed model for step edges.

The interpretation of atomically resolved constant-current STM topographies on  $\text{TiO}_2$  surfaces is complicated by strong electronic effects. Because  $\text{TiO}_2$  is an  $n$ -type semiconductor with a 3 eV band gap, empty states are normally imaged. The conduction band is dominated by Ti  $3d$  states which should give rise to a high tunneling probability and bright contrast on Ti sites. On the other hand, the anatase (101) surface is very corrugated and the twofold-coordinated oxygen atoms at the highest position could also be imaged bright. On rutile (110) the STM contrast is typically reversed to the physical topography under the usual tunneling conditions (positive sample bias of  $\sim 1.5$  V and tunneling current of  $\sim 1$  nA), and, despite their higher  $z$  position, twofold-coordinated oxygen atoms are imaged darker than titanium atoms.<sup>11</sup> The adsorbates on the step edges in Fig. 3 are located between the rows of bright atoms on the terrace. If the adsorbates are attached to Ti sites, the rows of bright terrace atoms will be at the location of the twofold-coordinated oxygens. Note, however, that the images in Fig. 3 have been taken with an unusually high tunneling current of 12 nA where the tip is expected to be rather close to the surface. Such extreme conditions can alter the image contrast on rutile (110).<sup>12</sup> The image in Fig. 4 was taken with a lower tunneling current of 1.23 nA. The bright spots on the terraces are found to be larger and elongated, possibly extending across the position of both the fivefold-coordinated Ti and the twofold-coordinated O atoms. Such an imaging behavior is not typically found on the rutile (110) surface. It may indicate a fundamental difference in the electronic structure of the two surfaces; possibly pointing towards a higher degree of covalent bonding in the case of anatase (101).

One of the major strengths of STM is the identification of defect structures that give rise to much of the interesting surface chemistry on transition-metal oxides. The preparation procedure used in this work (i.e., sputtering and anneal-

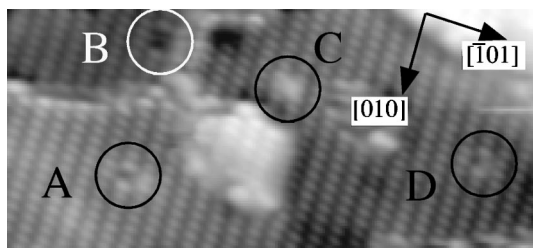


FIG. 4. STM image ( $V_{\text{sample}} = +1.22$  V,  $I_{\text{tunnel}} = 1.23$  nA,  $130 \times 60 \text{ \AA}^2$ ) of an anatase (101) surface. Four features could possibly be representative of oxygen vacancies; single black spots (A), double black spots (B), bright spots (C), and half black spots (D).

ing in UHV) gives rise to a few percent of oxygen vacancies on rutile (110).<sup>13</sup> These point defects have a dramatic effect on the surface chemistry and photocatalytic properties of rutile (110).<sup>13,2</sup> In STM they can be identified as small bright spots on dark rows.<sup>11,10</sup> Indicated in Fig. 4 are four types of imperfections on anatase (101) that could possibly be assigned to similar point defects. Without theoretical input it is hard to identify which of these features, if any, would be indicative of an oxygen vacancy. However, it is interesting that the concentration of all four types is rather low, far less than 1% of a monolayer. Either the anatase (101) surface is very stable against the loss of twofold-coordinated oxygen atoms, or STM is not capable of imaging such vacancies. The rather low surface free energy in the calculations seems to indicate a high stability of this surface. Electron-energy-loss spectra also point in this direction. Oxygen vacancies on rutile (110) give rise to a clear defect state in the band gap<sup>13</sup> which is virtually absent on anatase (101).<sup>14</sup>

These results are important for several reasons. First of all, they illustrate how to prepare anatase surfaces for atomic-level investigations. While the mineral crystal used in this work contains impurities in the bulk, it is perfectly suitable as a substrate for the homoepitaxial growth of high-quality anatase films. A similar approach has been successful for anatase (100) where the close lattice match between  $\text{SrTiO}_3(001)$  substrate has been exploited to grow and stabilize heteroepitaxial anatase films.<sup>7</sup> In this way all low-index faces of anatase will conceivably be amenable to surface science investigations. Secondly, these results strongly support the  $(1 \times 1)$  surface geometry predicted theoretically, and

provide a detailed model for the coordination of step atoms. This knowledge will be the starting point for any deeper understanding of adsorption and reaction processes at the molecular level. For example, the steric configuration determines largely if water adsorbs molecularly or dissociatively on rutile  $\text{TiO}_2$  surfaces.<sup>13</sup> Water binds molecularly to fivefold-coordinated Ti atoms, and dissociates by undergoing an H-O bond with neighboring twofold-coordinated oxygens. The relatively large distance between the Ti atoms on the terraces and the O atoms at the ridges of the zig-zags (Fig. 1) appears unfavorable for this dissociation pathway. The small concentration of defects on the terraces indicates a relatively low reactivity of the terraces; it is quite possible that reactions happen predominantly at the step edges. Third, the tunneling site in STM was identified, and a set of parameters was found that allows for a monitoring of both the surface oxygen and the titanium atoms. This is important for future experiments as it will permit the identification of adsorption sites directly from STM images.

In summary, this paper reports experimental results on the surface geometry and electronic structure of the  $\text{TiO}_2$  anatase (101) surface. An unreconstructed  $(1 \times 1)$  termination is obtained through sputtering and annealing in UHV. Atomically resolved STM images support a model for an autocompensated, bulk-terminated surface. Preferred step orientations have been identified. They contain fourfold-coordinated Ti atoms that are active centers for adsorption. Depending on the tunneling conditions, twofold-coordinated oxygen atoms can be distinguished in empty-states STM images. The surface is surprisingly stable and appears to have little tendency to form point defects.

This work was supported by NSF-CAREER, DoE-EPSCoR, and the PNNL-LDRD program. We thank Jeffrey E. Post from the Smithsonian Institution for lending us the mineral sample and R. Schmehl for useful discussions. The research described in this paper was performed at Tulane University and at the Environmental Molecular Sciences Laboratory, a national scientific user facility sponsored by the DOE Office of Biological and Environmental Research located at PNNL. PNNL is operated for the U.S. DOE by Battelle Memorial Institute under Contract No. DE-AC06-76RLO 1830.

\*Corresponding author: Ulrike Diebold; email: diebold@tulane.edu; fax: 504-862-8702.

<sup>1</sup> *Photocatalysis Fundamentals and Applications*, edited by N. Serpone and E. Pelizzetti (Wiley, New York, 1989).

<sup>2</sup> A. L. Linsebigler, G. Lu, and J. T. Yates, Jr., *Chem. Rev.* **95**, 735 (1995).

<sup>3</sup> B. O'Regan and M. Grätzel, *Nature (London)* **353**, 737 (1991).

<sup>4</sup> V. E. Henrich and P. A. Cox, *The Surface Science of Metal Oxides* (Cambridge University Press, Cambridge, 1994).

<sup>5</sup> A. Vittadini, A. Selloni, F. P. Rotzinger, and M. Grätzel, *Phys. Rev. Lett.* **81**, 2954 (1998).

<sup>6</sup> H. Onishi and Y. Iwasawa, *Surf. Sci. Lett.* **313**, 783 (1994).

<sup>7</sup> G. S. Herman, M. R. Sievers, and Y. Gao, *Phys. Rev. Lett.* **84**, 3354 (2000).

<sup>8</sup> R. Hengerer, B. Bolliger, M. Erbudak, and M. Grätzel, *Surf. Sci.* **400**, 162 (2000).

<sup>9</sup> J. P. LaFemina, *Crit. Rev. Surf. Chem.* **3**, 297 (1994); P. W. Tasker, *J. Phys. C* **12**, 4977 (1979).

<sup>10</sup> U. Diebold *et al.*, *Surf. Sci.* **411**, 137 (1998).

<sup>11</sup> U. Diebold, J. F. Anderson, K.-O. Ng, and D. Vanderbilt, *Phys. Rev. Lett.* **77**, 1322 (1996).

<sup>12</sup> O. Gülseren, R. James, and D. W. Bullett, *Surf. Sci.* **377-379**, 150 (1997); R. E. Tanner, M. R. Castell, and G. A. D. Briggs, *ibid.* **412**, 672 (1998).

<sup>13</sup> M. A. Henderson, *Surf. Sci.* **355**, 151 (1996); **319**, 315 (1994).

<sup>14</sup> M. A. Henderson (unpublished).

<sup>15</sup> G. S. Herman and Y. Gao (unpublished).